MIMO Capacity, Level Crossing Rates and Fades: The Impact of Spatial/Temporal Channel Correlation

Andrea Giorgetti, Peter J. Smith, Mansoor Shafi, and Marco Chiani

Abstract: **It is well known that Multiple Input Multiple Output (MIMO) systems offer the promise of achieving very high spectrum efficiencies (many tens of bit/s/Hz) in a mobile environment. The gains in MIMO capacity are sensitive to the presence of spatial and temporal correlation introduced by the radio environment. In this paper, we examine how MIMO capacity is influenced by a number of factors e.g., a) temporal correlation b) various combinations of low/high spatial correlations at either end, c) combined spatial and temporal correlations. In all cases, we compare the channel capacity that would be achievable under independent fading. We investigate the behaviour of "capacity fades," examine how often the capacity experiences the fades, develop a method to determine level crossing rates and average fade durations and relate these to antenna numbers. We also evaluate the influence of channel correlation on the capacity autocorrelation and assess the fit of a Gaussian random process to the temporal capacity sequence. Finally we note that the particular spatial correlation structure of the MIMO channel is influenced by a large number of factors. For simplicity, it is desirable to use a single overall correlation measure which parameterizes the effect of correlation on capacity. We verify this single parameter concept by simulating a large number of different spatially correlated channels.**

Index Terms: **MIMO systems, Shannon capacity, space-time correlation.**

I. INTRODUCTION

Since the pioneering work of Winters [1], Telatar [2], Foschini and Gans [3], Multiple Input Multiple Output (MIMO) systems have received considerable attention in recent years as they have the potential to provide quantum leaps in capacity [4]. The gains in MIMO shown in [3] are for independent fading amongst the antenna elements. More recently, several studies have addressed the issue of correlated fading, including work on measurements and models [5]–[10], the effects of correlation [5], [7], [11], [12] and large system results [13]–[15]. In order to fully evaluate the impacts of correlation on MIMO capacity, one needs to consider the combined effects of all sources of channel degradation pertinent to a MIMO channel, namely angle spread of the arriving multipath signal, Doppler spectrum and the delay power spectrum. In the open literature, there appear to be no expressions for a combined spectrum that take into account all of the three types of mobile channel spread mentioned above. If, however, the constituent spatial, temporal, and spectral correlations are assumed independent, then a combined correlation is simply the product of the constituent correlations. Abdi and Kaveh [8] have developed closed form expressions for spectral-temporal correlation that take into account various parameters of interest such as angle spreads at the base station and user end, array configurations, Doppler spreads, etc. They have used a von Mises distribution for the angles of arrival and departure. The wireless standards body 3GPP has published a standardized set of MIMO propagation models [9] that define key parameters and distributions needed to evaluate the combined spatial/temporal/spectral correlation function. In this paper, we have considered the standardized propagation model in [9] and only considered the effects of spatial and temporal correlation. The variation of capacity over time leads to the notion of finding periods of time where the capacity lies below a given value. We refer to these periods as "capacity fades" [16]. In the area of temporal capacity behaviour, we address the following issues:

- With temporal correlation only, how often does the capacity experience fades and what are their duration?
- Are the rates of occurrence of capacity fades and their durations influenced by antenna numbers?
- How do the answers to the above change with the introduction of varying amounts of spatial correlation?
- Can the temporal and spatial correlations be considered separable?
- What is the shape of the capacity autocorrelation function (ACF): How does it relate to the channel ACF and how does it change with antenna numbers?
- Can the temporal capacity sequence be modeled by a simple Gaussian process?

Although the area of correlated MIMO channels is now well studied [5]–[15], the temporal capacity behaviour under spatio-temporal correlation is not well known and provides the focus for this paper. By using a discrete time Gaussian process approximation for the capacity sequence (validated by simulations), we provide closed form expressions for the level crossing rates (LCR) and average fade durations (AFD) of the capacity. However, the closed form expressions require a knowledge of the correlation between successive capacity values. We show how this correlation can be approximated for single input multiple output (SIMO) and multiple input single output systems (MISO) systems. We also provide a standard time series model for the capacity sequence and show that an integrated autoregressive moving average (ARIMA) model can be fitted to the capacity sequence. We verify the accuracy of the ARIMA model by comparing the ACF's of the differentiated capacity sequence via simulation and prediction. Although it is conjectured that under certain correlation conditions the capacity process will be-

Manuscript received February 1, 2003.

A. Giorgetti and M. Chiani are with DEIS, University of Bologna, Viale Risorgimento 2, 40136 Bologna, Italy, email: {agiorgetti, mchiani}@deis.unibo.it.

M. Shafi is with Telecom New Zealand, PO Box 293, Wellington, New Zealand, email: Mansoor.Shafi@telecom.co.nz.

Peter J. Smith is with the Department of Electrical and Computer Engineering, The University of Canterbury, Private Bag 4800 Christchurch, New Zealand, email: p.smith@elec.canterbury.ac.nz.

1229-2370/03/$10.00

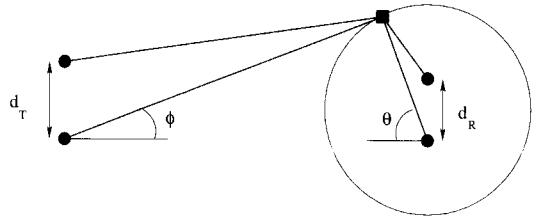

Fig. 1. The one-ring scatterers model for MIMO systems. The number of transmitting and receiving antennas are n_T and n_R, respectively.

come Gaussian for large systems, a proof is not attempted here.

We also consider the effect of spatial correlation on ergodic or mean capacity. It is known that MIMO capacity severely degrades with spatial correlation. Unfortunately, the correlations encountered are functions of many parameters, i.e., mean angles of arrival and departure, antenna spacings and layout, angle spreads, distributions of angles. It would be highly desirable to characterize the effect of the whole correlation structure on capacity with a single parameter that represents in some sense the overall channel correlation [17]. For example, if you wish to assess the effect of channel correlation on capacity variance, then it would be ideal to plot capacity variance against a single correlation measure. The alternative is to run many scenarios with no clear idea as to how to order the level of correlation. To date, such measures are little known and essentially adhoc, as in the "average" correlation used in [9]. In this area, we answer the following questions:

- Can a spatially correlated channel be described by a single parameter?
- How does mean capacity change with the single parameter given antenna numbers, signal-to-noise ratio (SNR), etc.?

In Section II, we describe the MIMO propagation model and show that temporal and spatial correlations may be treated independently. In Section III we investigate capacity fades for spatially/temporally correlated MIMO systems and fit a Gaussian random process to the temporal capacity sequence. The major part of Section IV is concerned with the development and comparison of single correlation parameters to describe the relationship between capacity and channel correlation. In Section V, we present numerical results in terms of capacity, level crossing rates, and average fade durations. In addition, extensive simulations are shown that support the use of a single correlation parameter to represent a complex physical scenario. Finally in Section VI, we give some conclusions.

II. MIMO CHANNEL MODEL

Let us consider a wireless system with (n_T, n_R) antennas as shown in Fig. 1 arranged as linear arrays at either end. The element spacing at the transmitter (TX) and the receiver (RX) end is denoted by d_T and d_R, respectively. We assume a flat fading channel model with possible correlation between the antenna array elements at both the base station and mobile station ends.

A. Propagation Model

The correlation model is derived from the well known model of a ring of scatterers surrounding a receive antenna array [5]. The model assumes the distribution of scatterers is such that angles of departure ϕ at the base station follow a Laplacian distribution, and a uniform distribution for arrival angles θ [9] at the mobile station. The distances d_T and d_R are assumed small relative to both the distance between the two ends of the communications link and the distance between the scatterers and the arrays. Hence, each transmitter illuminates the same set of scatterers. This leads to a separable correlation structure as discussed below. Let h_{mp} be the complex channel coefficient between the receiver m, $m = 1, \cdots, n_R$ and transmitter p, $p = 1, \cdots, n_T$, then the correlation between two coefficients is given by

$$\mathbb{E}\left[h_{m_1 p_1} h^*_{m_2 p_2}\right] = \mathbb{E}\left[e^{j\,2\pi \frac{d(p_1,p_2)\sin\phi}{\lambda}}\, e^{j\,2\pi \frac{d(m_1,m_2)\sin\theta}{\lambda}}\right], \tag{1}$$

where λ is the carrier wavelength, $d(m_1, m_2)$ is the distance between the receive antennas m_1 and m_2, $d(p_1, p_2)$ is the distance between transmit antennas p_1 and p_2, and $\mathbb{E}[\cdot]$ is mathematical expectation. The expectations are taken with respect to the random position of scatterers, i.e., with respect to the random variables ϕ and θ.

The MIMO channel is therefore characterized by the $n_R \times n_T$ channel matrix $\mathbf{H}$ with elements h_{ij}. In a rich scattered frequency non-selective environment, the elements of $\mathbf{H}$ are complex Gaussian random variables with unit energy and their time variations are governed by the Jakes [18] fading process. In this paper, we have not considered the key hole channels where the elements of $\mathbf{H}$ are products of two independent Gaussian random variables rather than single complex Gaussians. By stacking up the columns of $\mathbf{H}$, we can construct the channel vector $\mathbf{h} = vec(\mathbf{H})$ for this system as

$$\mathbf{h} = [h_{1,1} \cdots h_{n_R,1} \cdots h_{1,n_T} \cdots h_{n_R,n_T}]^T, \tag{2}$$

where $()^T$ denotes matrix transpose. Then the channel (spatial) correlation matrix is defined as

$$\mathbf{R} = \mathbb{E}\left[\mathbf{h}\mathbf{h}^\dagger\right], \tag{3}$$

where $()^\dagger$ is the transpose conjugate operator. Now, $\mathbf{R}$ can be found given the statistical distributions of ϕ and θ and by using (1) and (2) in (3). Usually, the channel correlations are separable or at least approximately so. For example in our model, the expectation in (1) is given by a product of correlations between antenna elements at the transmitter and receiver end respectively, i.e., $\rho^T_{p_1,p_2}\rho^R_{m_1,m_2}$ [5], [8], [9] where $\rho^R_{m_1,m_2} = \mathbb{E}\left[e^{j2\pi d(m_1,m_2)\sin\theta/\lambda}\right]$.

Let us now define the symmetrical correlation matrices at the transmitter and receiver as $\mathbf{\Psi}_T = \left[\rho^T_{p,q}\right]_{n_T \times n_T}$ and $\mathbf{\Psi}_R = \left[\rho^R_{p,q}\right]_{n_R \times n_R}$. Then it can be shown that under the antenna element spacing and other conditions described above, it is possible to write [5], [8], [9]:

$$\mathbf{R} = \mathbf{\Psi}_T \otimes \mathbf{\Psi}_R, \tag{4}$$

where $\otimes$ is the Kronecker product. This is true in our model and allows us to independently vary correlation at either end and examine the consequential impact on capacity. Various measurements have been presented in the literature which support the

accuracy of the Kronecker form of the correlation matrix, for example [10].

Since we want to take into account not only spatial but also temporal correlation, we assume that the time variations of the channel coefficients in $\mathbf{H}$ are governed by the well known Jakes fading process [18]. So in the following, we use $\mathbf{H}$ when we consider only spatial correlation and $\mathbf{H}(t)$ for both spatial and temporal behaviour.

In conclusion, we can consider both temporal and spatial correlation and, by varying the maximum Doppler frequency f_D, element spacings and mean angles of arrival/departure, various scenarios of high and low correlation can be simulated.

B. Separability of Spatio/Temporal Correlations

Let us consider the vector $\mathbf{u} = vec(\mathbf{U})$ obtained by taking the columns of a $n_R \times n_T$ matrix $\mathbf{U}$ of zero-mean independent and identically distributed (i.i.d) complex Gaussian entries with unit energy. For the purpose of simulation, given the correlation matrix $\mathbf{R}$, the correlated channel coefficients $\mathbf{h}$ are simply obtained from the vector $\mathbf{u}$ by means of

$$\mathbf{h} = \mathbf{\Psi}\,\mathbf{u}, \tag{5}$$

where $\mathbf{\Psi} = [\psi_{ij}]$ is the square root of the correlation matrix of $\mathbf{h}$ [5], i.e.,

$$\mathbf{R} = \mathbf{\Psi} \cdot \mathbf{\Psi}^{\dagger}, \tag{6}$$

Now, introducing temporal correlation between the i$-th$ element of $\mathbf{u}(t)$ and the i$-th$ element of $\mathbf{u}(t-\tau)$, for the elements of $\mathbf{h}(t)$ we have

$$\begin{aligned}\mathbb{E}[h_i(t)h_i^*(t-\tau)] &= \mathbb{E}\left[\sum_j \sum_k \psi_{ij}\,\psi_{ik}^*\,u_j(t)u_k^*(t-\tau)\right] \\ &= \sum_j \sum_k \psi_{ij}\,\psi_{ik}^*\,\mathbb{E}[u_j(t)u_k^*(t-\tau)].\end{aligned} \tag{7}$$

But the elements of $\mathbf{u}(t)$ are independent, so only one sum survives

$$\mathbb{E}[h_i(t)h_i^*(t-\tau)] = \sum_j \psi_{ij}\,\psi_{ij}^*\,\mathbb{E}[u_j(t)u_j^*(t-\tau)]. \tag{8}$$

Now, assuming that all the elements $u_j(t)$ have the same temporal correlation $\rho_u(\tau)$, i.e.,

$$\rho_u(\tau) = \mathbb{E}[u_j(t)u_j^*(t-\tau)] \quad \forall j = 1 \cdots n_R \cdot n_T. \tag{9}$$

We obtain

$$\begin{aligned}\mathbb{E}[h_i(t)h_i^*(t-\tau)] &= \rho_u(\tau) \cdot \sum_j \psi_{ij}\,\psi_{ij}^* \\ &= \rho_u(\tau) \cdot [\mathbf{\Psi} \cdot \mathbf{\Psi}^{\dagger}]_{ii} = \rho_u(\tau).\end{aligned} \tag{10}$$

This proves that the spatial correlation does not alter the temporal correlation already present between the elements of $\mathbf{u}(t)$ and $\mathbf{u}(t-\tau)$.

Therefore, under the assumption that all the channels experience the same temporal correlation (this is a quite reasonable assumption), it is always possible to simulate a MIMO channel starting from spatially independent channels $\mathbf{U}(t)$ with a prescribed temporal correlation and, subsequently, introducing the spatial correlation by means of (5) in order to obtain a spatio/temporal correlated channel $\mathbf{H}(t)$. To be specific, we generate $n_R \times n_T$ independent time varying Gaussian processes using the Jakes-like generator in [19]. At each time point, t, the $n_R \times n_T$ Gaussians are stored in a channel matrix $\mathbf{U}(t)$. Spatial correlation is then induced by pre and post multiplication giving the sequence $\mathbf{H}(t) = \mathbf{\Psi}_R^{\frac{1}{2}}\mathbf{U}(t)\mathbf{\Psi}_T^{\frac{1}{2}}$. Note that this induces the same correlation structure as (5) and is more compact [5].

III. MIMO CAPACITY: TEMPORAL BEHAVIOUR

We consider a single user $n_T \rightarrow n_R$ MIMO system operating in a correlated fading environment discussed in Section II. The received signal, $\mathbf{r}$, is given by

$$\mathbf{r} = \mathbf{H}\,\mathbf{s} + \mathbf{n}, \tag{11}$$

where $\mathbf{r}$ is the $n_R \times 1$ received signal, $\mathbf{s}$ is the $n_T \times 1$ transmitted signal, and $\mathbf{n}$ is an $n_R \times 1$ vector of i.i.d additive white Gaussian noise terms normalized so that the elements have unit magnitude variance. The total power of $\mathbf{s}$ is constrained to P. $\mathbf{H}$ is the $n_R \times n_T$ channel matrix. Assuming equal power uncorrelated sources (optimum for the case when the transmitter does not know the channel or the channel statistics), the capacity is given by [3]

$$C = \log_2 \det\left(\mathbf{I}_{n_R} + \frac{P}{n_T}\mathbf{H}\mathbf{H}^{\dagger}\right) \text{ bit/s/Hz}. \tag{12}$$

If the channel is known, then waterfilling can be used [2]. If only the channel statistics are known through covariance feedback, then improvements over equal power allocation are also possible [20], [21]. Note that in all this work, we assume the "quasi-static" case [3] where the channel varies randomly from burst to burst. Within a burst, the channel is assumed fixed and it is also assumed that sufficient bits are transmitted for the standard infinite time horizon of information theory to be meaningful.

The capacity formula is now extremely well-known and the simple process of replacing $\mathbf{H}$ by a sequence of spatio-temporally correlated channel matrices $\mathbf{H}(i)$ for $i = 1, 2, \cdots$ results in a temporal sequence of capacity values. The modelling of the channel matrices is described in Section II.

A. Level Crossing Rates and Fade Durations

It is now reasonably well known that for independent fading, the capacity of MIMO systems is approximately Gaussian even for small numbers of antennas. For larger numbers, the approximation improves and suitably standardized (see below), the capacity converges to the Gaussian distribution as $n_R \rightarrow \infty, n_T \rightarrow \infty$, and the ratio n_R/n_T tends to a constant [22]–[26]. It is sensible therefore to investigate whether the temporally (and spatially) correlated sequence of capacity values might also be well approximated by a Gaussian sequence.

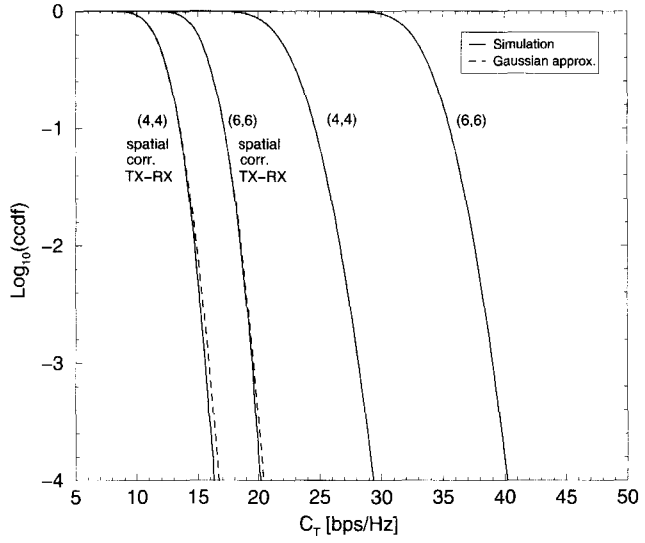

Fig. 2. Complementary cdf (ccdf) of the capacity, (4,4) and (6,6) MIMO for $P = 20$dB, with and without spatial correlation (continuous line) and the capacity ccdf predicted with the Gaussian assumption.

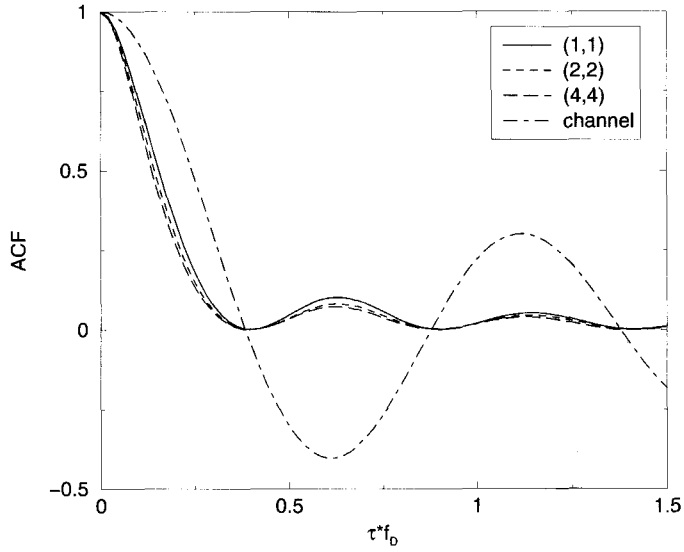

Fig. 3. Normalized ACF of the capacity in spatially uncorrelated channels with $P = 20$dB.

Whether the Gaussian approximation is accurate for correlated fading scenarios is less well-known. Hence in Fig. 2, we compare the complementary cumulative distribution function (ccdf) of the data with a Gaussian ccdf with the same mean and variance. The correlation scenarios used are described in Section V and the parameters given in Table I. The agreement is excellent and we proceed to investigate whether the temporal behaviour can also be approximated using Gaussian process results.

In order to investigate the temporal behaviour of the capacity, we focus on level crossing rates across a level C_T (denoted $LCR(C_T)$), and average fade durations (periods of time spent with $C < C_T$ denoted $AFD(C_T)$). For any discrete time Gaussian model, the LCR can be calculated as shown in APPENDIX A. We state the result below. Let ρ_c be the correlation between successive capacity values, μ be the mean capacity, and σ^2 the capacity variance. Defining the standardized capacity values as $\tilde{C} = (C - \mu)/\sigma$, we can express the LCR as:

$$LCR(\tilde{C_T}) = F(\tilde{C_T}) - \int_{-\infty}^{\tilde{C_T}} f(x) F\left(\frac{\tilde{C_T} - \rho_c x}{\sqrt{1-\rho_c^2}}\right) dx, \quad (13)$$

where $f(x)$ and $F(x)$ are the density and distribution function respectively of the standard Gaussian distribution. Note that this only requires the correlation parameter ρ_c. In order to model the capacity sequence more completely and obtain information beyond LCR's, we could attempt to fit a particular model, perhaps a Gaussian ARIMA(p,d,q) model, to the capacity sequence. This is briefly investigated in item III-D below. After the evaluation of the LCR, it can be related to the AFD using the result [18]

$$AFD(\tilde{C_T}) = \frac{F(\tilde{C_T})}{LCR(\tilde{C_T})}. \quad (14)$$

In Section V, we investigate how closely these simple Gaussian process approximations match our discrete time simulations. In APPENDIX B, we give another approach to computing the LCR based on a continuous time Gaussian model for the capacity sequence.

B. Autocorrelation Functions

Next, we take a look at the relationship between the temporal behaviour of the channel and the capacity sequence itself.

In Fig. 3, the normalized ACF $\rho_c(\tau)$ of the capacity, for different systems for a SNR of 20dB, is reported as a function of the normalized time-lag τf_D and compared to that of the channel ($J_0(2\pi\tau f_D)$), where f_D is the doppler frequency, $\tau = kT$, k is the time index, and T is the burst duration. In the following, we choose $f_D T = 0.02$. It is interesting to note that when the ACF of the channel crosses zero, the ACF's of the capacities are zero. This is due to the fact that each channel is complex Gaussian: therefore, if we consider a MIMO channel at different instants with a time-lag Δt such that the ACF of the channels are zero, the two matrices $\mathbf{H}(t)$ and $\mathbf{H}(t + \Delta t)$ have independent entries, leading to independent capacities. In addition, the peaks of the capacity ACF are given by the locations of the turning points in the channel ACF. Such a clear and simple relationship between the channel and the capacity ACF's is perhaps a little surprising given the complexity of the capacity as a function of the channel. We also note that for the systems considered, the ACF has only a small dependence on the number of antennas, even if a reduction of the amplitude of the oscillations can be observed for higher order systems with equal number of transmit and receive antennas.

C. Approximation of the ACF, LCR and AFD for SIMO and MISO systems

Now, let us consider a SIMO system $(1, n)$ with vector channel $\mathbf{h} = [h_1, h_2, \cdots, h_n]^T$ and complex channel gains $h_l = h_l^I + j h_l^Q$, the capacity formula (12) reduces to

$$C = \log_2(1 + P\,\mathbf{h}^\dagger \mathbf{h}) \quad \text{bit/s/Hz}, \quad (15)$$

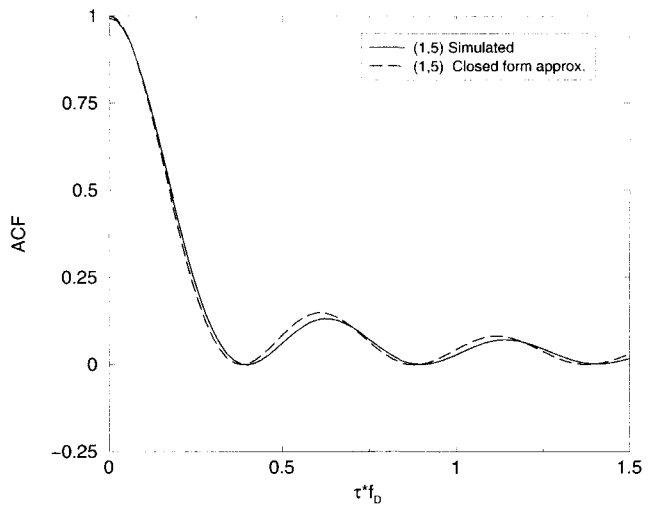

Fig. 4. Comparison of the simulated ACF at $P = 30$dB with that predicted by means of the closed form approximation derived in Section III-C.

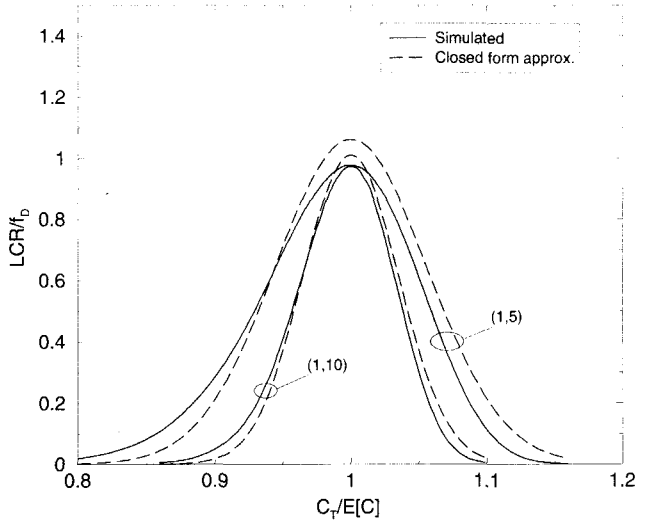

Fig. 5. Comparison of the simulated LCR at $P = 30$dB with that predicted by means of the closed form approximation derived in Section III-C.

where $X \triangleq \mathbf{h}^{\dagger}\mathbf{h}$ is a central chi-square distributed random variable (r.v.) with $2 \times n$ degrees of freedom, i.e., $X \sim \chi^2_{2n}$. In order to evaluate the ACF of the capacity in a closed form, we consider the case where the SNR is high ($P >> 1$), so that

$$C \approx \overline{C} = \log_2(P\,X). \tag{16}$$

If we consider time-correlated channels, replacing the vector $\mathbf{h}$ with a sequence of channel vectors $\mathbf{h}(i)$ for $i = 1, 2, \cdots$ results in a temporal sequence of capacity values $\overline{C}(i)$. The ACF $R_{\overline{c}}(k)$ of the capacity in this case is

$$\begin{aligned} R_{\overline{c}}(k) &= \mathbb{E}\left[\overline{C}(i)\overline{C}(i-k)\right] \\ &= \mathbb{E}\left[\log_2(P\,X(i))\log_2(P\,X(i-k))\right]. \end{aligned} \tag{17}$$

In particular, we are interested in the evaluation of the normalized ACF

$$\rho_{\overline{c}}(k) = \frac{R_{\overline{c}}(k) - \mu^2_{\overline{c}}}{\sigma^2_{\overline{c}}}, \tag{18}$$

where $\mu_{\overline{c}}$ and $\sigma^2_{\overline{c}}$ are the mean value and the variance of the capacity, respectively. Therefore, the evaluation of the normalized ACF (18) requires the evaluation of

$$R_{\overline{c}}(k) - \mu^2_{\overline{c}} = \mathbb{E}\left[\log_2 X(i)\log_2 X(i-k)\right] - \left(\mathbb{E}\left[\log_2 X(i)\right]\right)^2, \tag{19}$$

where [27]

$$\mathbb{E}\left[\log_2 X(i)\right] = \frac{\psi(n)}{\ln 2}, \tag{20}$$

and $\psi(\cdot)$ is the *Euler's digamma function* [28, eq. 8.36]. In APPENDIX C, the first expectation in (19) is evaluated as:

$$R_{\overline{c}}(k) = \frac{\rho^2_h(k)}{n}\,{}_3F_2\left(1,1,1;2,n+1;\rho^2_h(k)\right) + \psi^2(n), \tag{21}$$

where ${}_3F_2(\cdot;\cdot;\cdot)$ is the *generalized hypergeometric function* [28, eq. 9.14] and $\rho_h(k)$ is the normalized ACF of the underlying Gaussian channel (see APPENDIX C). Therefore, considering that $\sigma^2_{\overline{c}} = \psi'(n)/\ln^2(2)$, the normalized ACF of the capacity at high SNR becomes:

$$\rho_{\overline{c}}(k) = \frac{\rho^2_h(k)\,{}_3F_2\left(1,1,1;2,n+1;\rho^2_h(k)\right)}{n\,\psi'(n)}. \tag{22}$$

In a similar manner, we could proceed for a $(n,1)$ MISO system obtaining the same formula. Note that this formula is valid whatever the ACF of the channel is.

Now, starting from (22), we can evaluate not only the ACF, but also the level crossing rate (and consequently the AFD) by using (13) and substituting ρ_c with $\rho_{\overline{c}}(1)$ which depends only on $\rho_h(1)$. In Fig. 4, the comparison between the simulated ACF at $P = 30$dB with that predicted by means of the closed form approximation (22) for a MIMO $(1,5)$ system is reported. Note that at high SNR ($P = 30$dB), our formula works very well.

In Fig. 5, the comparisons between the simulated LCR at $P = 30$dB with that predicted by means of (13) and (22) for $(1,5)$ and $(1,10)$ systems are reported. Note that at high SNR ($P = 30$dB) and for high-diversity systems, our approach works very well. Furthermore, the approximation becomes good when the number of antennas increases. Note however that the capacity (15) does not tend to a Gaussian r.v. for large n, but rather the logarithm of a Gaussian. This is because only one of the array dimensions is being increased.

D. Model Fitting

Here, we investigate the possibility of fitting standard time series models to the capacity sequence. We consider an example (4,4) MIMO system with $P = 20$dB, no spatial correlation and $f_D T = 0.02$. The sequence is generated as described in Section II-B. A discrete time simulation of 300,000 points was used giving the sequence $\{C(1), C(2), \cdots\}$ and an autoregressive integrated moving average (ARIMA) model [29] was fitted. We used the most basic approach to model fitting [29]: First, differencing the sequence until the ACF decayed away fairly rapidly and then selecting the order of the AR and MA components by inspecting the ACF and partial autocorrelation function (PACF).

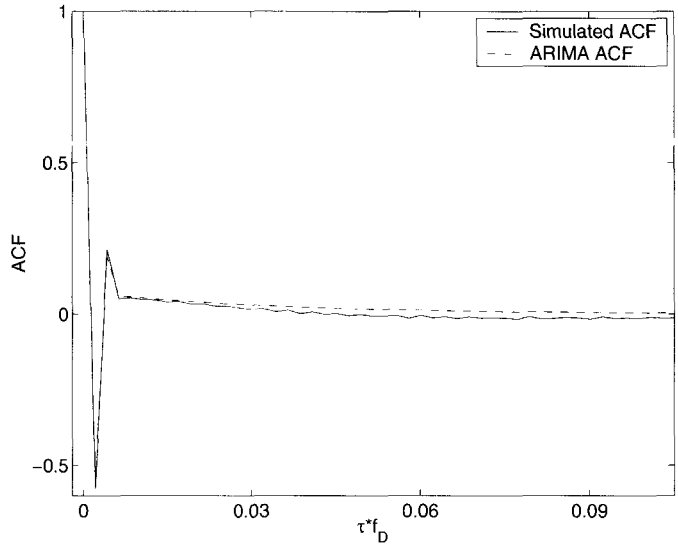

Fig. 6. ACF of the capacity second difference ($\nabla^2 C$) in a spatially uncorrelated (4,4) MIMO channel for $P = 20$dB.

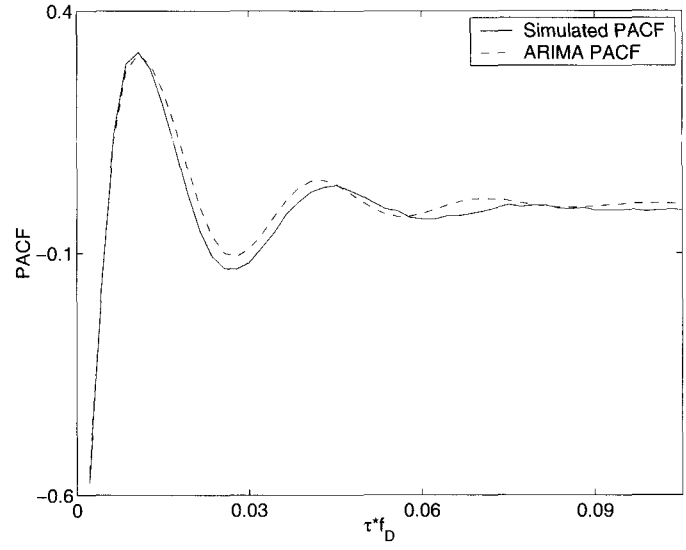

Fig. 7. PACF of the capacity second difference ($\nabla^2 C$) in a spatially uncorrelated (4,4) MIMO channel for $P = 20$dB.

Parameter estimation was possible by maximum likelihood due to the Gaussian assumption for the process. This approach led to the ARIMA(1,2,3) model given by

$$\begin{aligned}&\nabla^2 C(i) - 0.9397\,\nabla^2 C(i-1)\\&= \epsilon(i) - 1.9425\,\epsilon(i-1) + 1.3502\,\epsilon(i-2) 0.2716\,\epsilon(i-3),\end{aligned} \tag{23}$$

where $\{\epsilon(i)\}$ is a white Gaussian noise sequence and ∇ is the difference operator, such that

$$\nabla^2 C(i) = \nabla(C(i) - C(i-1)) = C(i) - 2C(i-1) + C(i-2). \tag{24}$$

In Figs. 6 and 7, we plot the simulated ACF and PACF of $\nabla^2 C(i)$ and the ACF/PACF given by the ARIMA model. As can be seen, the agreement is reasonable so that Gaussian random processes may be useful, not only in evaluating LCR's and AFD's, but also in characterizing more detailed temporal behaviour. Note that formal tests of the ARIMA model were performed, but predictably (as we have 300,000 data points), they strongly rejected the model. This is due to the well known statistical property that even extremely accurate models are rejected given enough data.

IV. MIMO CAPACITY: PARAMETERIZING THE EFFECTS OF SPATIAL CORRELATION

To completely define the spatial correlation structure, we must specify the angular p.d.f's of ϕ and θ. We assume that ϕ follows a Laplacian distribution [9]

$$f(\phi) = \frac{k}{2(1 - e^{-k\pi})} e^{-k|\phi - \mu|} \quad \phi \in [-\pi + \mu, \pi + \mu), \tag{25}$$

where μ is the average angle of arrival and k is a parameter related to the angle spread σ, i.e., the standard deviation of ϕ: $\sigma = [(2 - e^{-k\pi}(2 + 2k\pi + k^2\pi^2)/(k^2(1 - e^{-k\pi}))]^{\frac{1}{2}}$.

For $k = 0$ (isotropic scattering) we have $f(\phi) = 1/2\pi$, while for $k = \infty$ the Laplacian distribution becomes a Dirac delta function, concentrated at μ. With this assumption, the elements of the correlation matrix $\mathbf{\Psi}_T$ need to be evaluated by numerical integration. At the receiver, we assume a uniform angle of arrival so that $f(\theta) = 1/2\pi$, and the correlation matrix $\mathbf{\Psi}_R$ has elements

$$\rho^R_{p,q} = J_0\left(2\pi \frac{d(p,q)}{\lambda}\right). \tag{26}$$

In this section we define two different parameters that can be used to characterize the amount of spatial correlation. Our aim is to reparameterize the correlation which can be a function of many parameters: Mean angles of arrival and departure, antenna spacings and layout, angle spreads, distributions of angles, etc. Hence, we attempt to measure the overall correlation by a single parameter which accurately characterizes the effect of correlation on capacity. Uses of this single parameter would include plots of mean capacity, outage capacity, or capacity variance against the single correlation measure.

A. A Norm of the Correlation Matrix $\mathbf{R}$

In order to quantify the amount of spatial correlation introduced by the propagation scenario and the geometry of the antennas, we define a norm $\alpha_p = \|\mathbf{R}\|_p$ for $p \in \{1, 2, \cdots \infty\}$ as a combination of the off-diagonal elements of the correlation matrix $\mathbf{R} = [r_{ij}]$ given by

$$\alpha_p = \|\mathbf{R}\|_p \triangleq \left(\frac{\sum_{i \neq j} |r_{ij}|^p}{n^2 - n}\right)^{\frac{1}{p}}, \tag{27}$$

where $n = n_T \cdot n_R$. With this definition, $\|\mathbf{R}\|_1$ is the average of the off-diagonal elements, while $\|\mathbf{R}\|_\infty = \max_{i \neq j}(|r_{ij}|)$ is simply the maximum value. This measure is in the range between 0 and 1 and, in fact, when $\mathbf{R} = \mathbf{I}_n$ (uncorrelated case) we have $\|\mathbf{R}\|_p = 0\ \forall p$, while in the totally correlated case $\mathbf{R} = \mathbf{1}_n$

($\mathbf{1}_n$ is a $n \times n$ matrix of all ones) we have $\|\mathbf{R}\|_p = 1\ \forall p$. Note that $\alpha_1, \alpha_2, \alpha_3, \cdots$ put successively more weight on the larger correlations.

B. The determinant of $\mathbf{\Psi_T}$ and $\mathbf{\Psi_R}$

Let us start from the capacity formula (12) that for the correlated case can be expressed as

$$\begin{aligned} C &= \log_2 \det\left(\mathbf{I}_{n_R} + \frac{P}{n_T}\mathbf{H}\mathbf{H}^\dagger\right) \\ &\sim \log_2 \det\left(\mathbf{I}_{n_R} + \frac{P}{n_T}\mathbf{\Psi}_R\mathbf{U}\mathbf{\Psi}_T\mathbf{U}^\dagger\right), \end{aligned} \tag{28}$$

where $X \sim Y$ indicates that the random variables X and Y have the same distribution and $\mathbf{U}$ is the i.i.d. Gaussian matrix defined in Section II-B.

Based on this result, another possible correlation measure is suggested considering the capacity for high values of the SNR

$$\begin{aligned} C \approx \overline{C} &= \log_2 \det\left(\frac{P}{n_T}\mathbf{\Psi}_R\mathbf{U}\mathbf{\Psi}_T\mathbf{U}^\dagger\right) \\ &= n_R \log_2\left(\frac{P}{n_T}\right) + \log_2 \det(\mathbf{U}\mathbf{U}^\dagger) \\ &\quad + \log_2\left[\det(\mathbf{\Psi}_R)\det(\mathbf{\Psi}_T)\right]. \end{aligned} \tag{29}$$

Therefore, for high SNR, the capacity in the correlated case is approximately equal to the capacity of the uncorrelated case plus a term $\log_2(\alpha)$ where $\alpha \triangleq \det(\mathbf{\Psi}_R)\det(\mathbf{\Psi}_T)$.

Hence, at high SNR, α represents the entire contribution of the spatial correlation to the capacity. Note that the derivation of $\overline{C}$ assumed that $n_R \leq n_T$. However, it is straightforward to modify the approach for $n_R > n_T$ and this leads to the same parameter α. In Section V, we investigate the dependence of the average capacity $\mathbb{E}[C]$ and the 10% outage capacity $C_{0.1}$ as a function of this parameter even for low SNR.

In addition to the two correlation parameters defined above, we also tried the correlation parameter defined by Mestre *et al.* [12] (extended to the two-sided correlation scenario) and the approximate mean capacity formula of Martin and Ottersten [15]. Neither metric appeared to capture the effects of correlation as well as α or α_3. Hence, these results are not presented here.

As a reference, it is easy to prove that the expected value $\mathbb{E}[C]$ of the capacity for the totally correlated case ($\mathbf{R} = \mathbf{1}_{n_T n_R}$) is the same as that for a SISO channel but with a SNR P multiplied by n_R, i.e.,

$$\mathbb{E}[C] = -\frac{e^{1/P\,n_R}}{\ln(2)} \cdot \mathrm{Ei}\left(-\frac{1}{P\,n_R}\right) \quad \text{bit/s/Hz}, \tag{30}$$

where Ei is the *exponential integral function* [28]. At the other extreme, the mean capacity for the uncorrelated case is given by Telatar [2].

V. NUMERICAL RESULTS

The simulation of MIMO channels with temporal correlation only requires the generation of multiple complex waveforms satisfying the following conditions. First, the real and imaginary parts are independent zero-mean random Gaussian processes with identical ACF's. Second, the complex waveforms are independent so that the crosscorrelation function between any two waveforms is zero. Therefore, the following results are obtained using a method that improves Jakes' simulator in order to generate multiple Rayleigh fades, which agree with the theoretical hypothesis above mentioned [19]. As an example, employing $N_o = 16$ oscillators, we can generate 72 different channel waveforms (needed for a MIMO system with 6 transmitting and receiving antennas) with a crosscorrelation function whose modulus is less than 0.07.

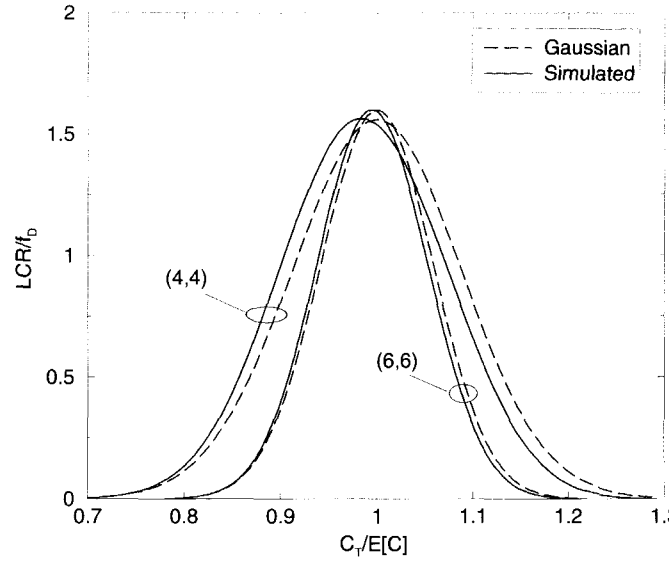

Fig. 8. LCR of the capacity without spatial correlation: Comparison between Gaussian process approximation and simulation for P = 20dB.

Now, let us start by examining the numerical results on the impact of spatial and temporal correlations on the capacity. Fig. 8 shows the comparison of the simulated LCR of the capacity for (4,4) and (6,6) systems with that predicted by means of the Gaussian process approximation discussed in Section III. The LCR (13) is divided by the burst duration T and normalized by the Doppler frequency f_D, while in the abscissa there is the capacity level C_T normalized by the mean $\mathbb{E}[C]$. For this simulation and for what follows the product, $f_D T$ is equal to 0.02. Note that the analytical model fits very well demonstrating the validity of the Gaussian approximation for the capacity, not only for the first-order analysis [23], but also for the process over time.

The normalized (with respect to f_D) LCR and the normalized AFD of the capacity for different MIMO systems with P = 20dB are reported in Fig. 9 and Fig. 10, respectively. Note that in the abscissa there is the capacity fade probability or outage probability $P_{out} = \mathbb{P}\{C < C_T\}$. This kind of normalization allows us to better compare the burstiness of different systems at the same outage probability. For example, we can fix P_{out} = 0.1 and look vertically from 0.1 to see the LCR's for different systems across the threshold C_T defined by $\mathbb{P}\{C < C_T\} = 0.1$. Hence, our comparison is of the LCR's across the "equivalent"

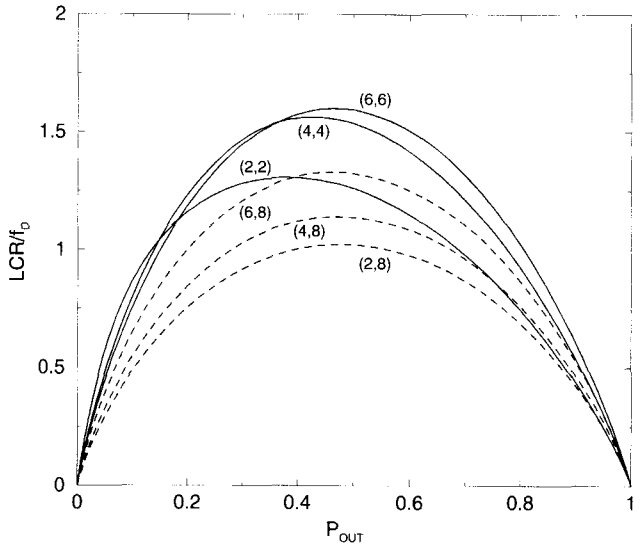

Fig. 9. LCR of the capacity without spatial correlation for different MIMO systems with $P = 20$dB. Note that in the abscissa there is the outage probability.

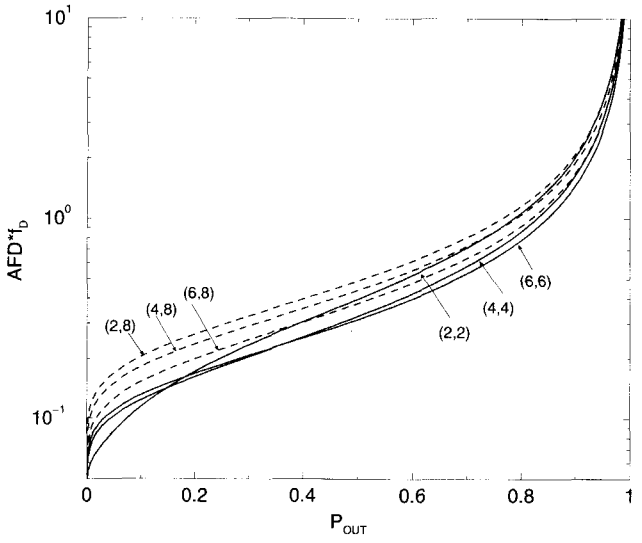

Fig. 10. AFD of the capacity for the same systems shown in Fig. 9.

threshold for each system. The AFD curves are easily evaluated taking into consideration formula (14). If we look at low P_{out}, systems with high receive diversity, i.e., a high n_R/n_T ratio, have low LCR and high AFD. Also at low P_{out}, low AFD can be obtained with low numbers of antennas at both the transmitter and receiver.

Now, introducing spatial correlation at transmit and receive antennas as described in Section II, we evaluate its impact on the first and second-order statistical properties of the capacity. Here, we consider equally spaced elements at the TX as well as the RX and three different cases of high spatial correlation: At the TX, at the RX, and both TX-RX. For the correlation at TX, we have considered three parameters: The average angle of arrival (AOA) μ, the angle spread σ, and the distance between the transmit antennas d_T. For the correlation at the RX, we consider only the antenna spacing d_R and a uniform distribution of

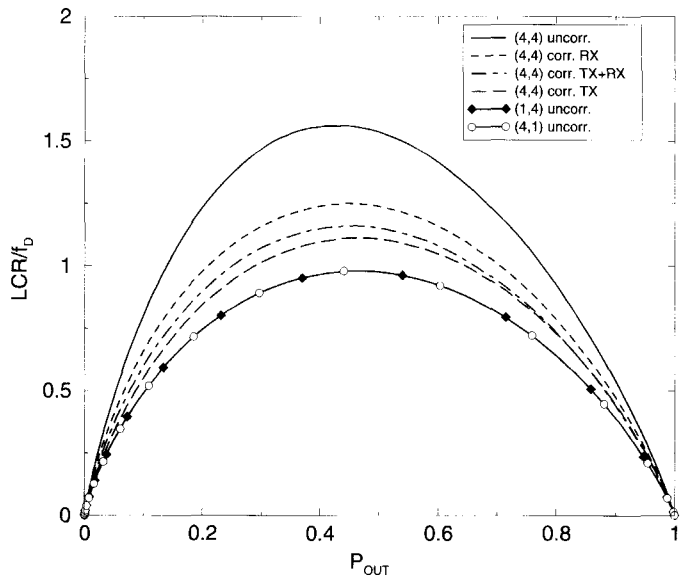

Fig. 11. LCR for different spatial correlation at TX and RX with $P = 20$dB.

Table 1. The three different scenarios considered in Figs. 2 and 11.

	σ	μ	d_T	d_R
RX	20°	0°	10λ	0.2λ
TX	5°	90°	5λ	λ
TX-RX	5°	90°	5λ	0.2λ

the AOA that allow us to use a modified Jakes' simulator for the generation of the channel (remembering that the Jakes' model is based on the assumption of uniform scatterers on a circle around the RX). In Table 1, the parameters employed in the following results for the three cases are summarized.

In Fig. 2, we plot the complementary cumulative distribution function (ccdf) $\mathbb{P}\{C > C_T\}$ of the capacity for (4,4) and (6,6) systems, respectively, with and without spatial correlation, compared with the Gaussian approximation to the capacity distribution and for a signal-to-noise ratio of 20dB. As for the Rayleigh and Ricean cases already studied in [23], the Gaussian approximation does remarkably well considering the high spatial correlations corresponding to the TX-RX scenario. The strong impact of the spatial correlation is clear, reducing the capacity by around 40%: A (6,6) system with this spatial correlation is worse than an uncorrelated (4,4).

Concerning the impact of the spatial correlation on the second-order statistics of the capacity, Fig. 11 shows the LCR for a (4,4) system in the three correlated scenarios described above and with $P = 20$dB. As a reference, the LCR's for (4,4), (4,1), and (1,4) systems without spatial correlation are reported. For a fixed P_{out}, the spatial correlation reduces the LCR and therefore increases the average duration of capacity fades. For the scenarios considered here, the impact of the correlation at TX seems to be less than that at RX.

Now, let us examine the numerical results on the impact of the spatial correlation on the mean capacity $\mathbb{E}[C]$ and the 10% outage capacity $C_{0.1}$ via the two different parameters α_p and α given in Section IV. In order to investigate the capacity degra-

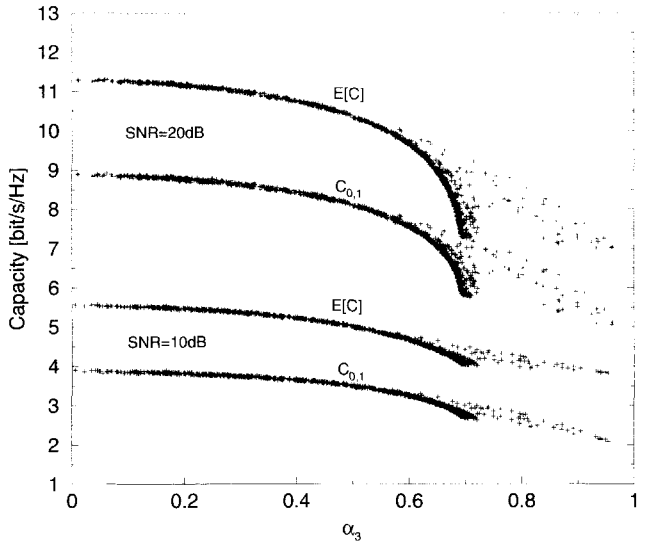

Fig. 12. $\mathbb{E}[C]$ and $C_{0.1}$ vs. α_3 for a (2,2) MIMO system at different SNRs.

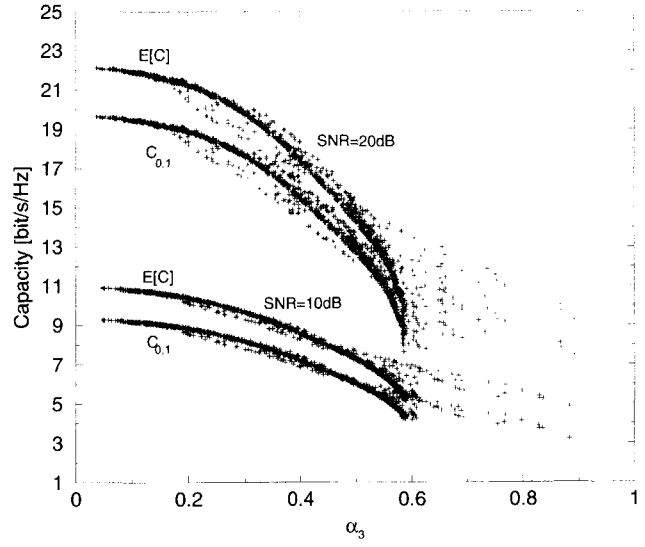

Fig. 13. $\mathbb{E}[C]$ and $C_{0.1}$ vs. α_3 for a (4,4) MIMO system at different SNRs.

Table 2. Spatial correlation parameters for different scenarios.

Scenario				(2,2)		(4,4)	
σ	μ	d_T	d_R	α_3	$\log_{10}\alpha$	α_3	$\log_{10}\alpha$
5°	0°	5λ	λ	0.19	-0.042	0.13	-0.14
20°	0°	λ	0.5λ	0.26	-0.077	0.18	-0.25
20°	0°	10λ	0.2λ	0.45	-0.23	0.30	-2.02
45°	45°	λ	0.2λ	0.47	-0.28	0.32	-2.19
20°	90°	λ	0.5λ	0.62	-0.70	0.50	-2.46
5°	90°	5λ	λ	0.68	-1.30	0.55	-4.61
5°	90°	5λ	0.2λ	0.78	-1.51	0.65	-6.56

dation as a function of these parameters, we generate up to 2000 scenarios by choosing randomly the 4-tuple (σ, μ, d_T, d_R) for a fixed n_T, n_R, and SNR P. Then, for each scenario, we evaluate α_p, α and we estimate $\mathbb{E}[C]$ and $C_{0.1}$ from 10000 instances of the channel matrix $\mathbf{H}$. After a simulation campaign, we chose $p = 3$ as the best value for $\|\mathbf{R}\|_p$, since it gave the best accuracy in mean capacity prediction. Since $\alpha_1, \alpha_2, \alpha_3, \cdots$ put successively more weight on the large correlations, it is unsurprising that α_2 and α_3 outperform α_1. However, the gains in using α_n as n increases further then begin to drop.

In Table 2, there are some example scenarios and the corresponding values α_3 and α for (2,2) and (4,4) systems.

Fig. 12 displays $\mathbb{E}[C]$ and $C_{0.1}$ for a (2,2) system at different SNRs as a function of α_3. The figure shows that the capacity can be predicted accurately when the parameter is in the range from 0 to 0.6 at 10dB and 0 to 0.5 at 20dB. Fig. 13 displays $\mathbb{E}[C]$ and $C_{0.1}$ for a (4,4) system at different SNRs as a function of α_3. The figure shows an increase in dispersion of the curves, especially at $P = 20$dB, so that the capacity can be predicted with less accuracy. Even so, the results are still good.

The capacity for a (2,2) system for different SNRs as a function of α is reported in Fig. 14. The parameter α seems to be extremely good in predicting the capacity of a (2,2) system, giving virtually a direct correspondence between α, $\mathbb{E}[C]$, and $C_{0.1}$. The same analysis for a (4,4) system is plotted in Fig. 15. Here,

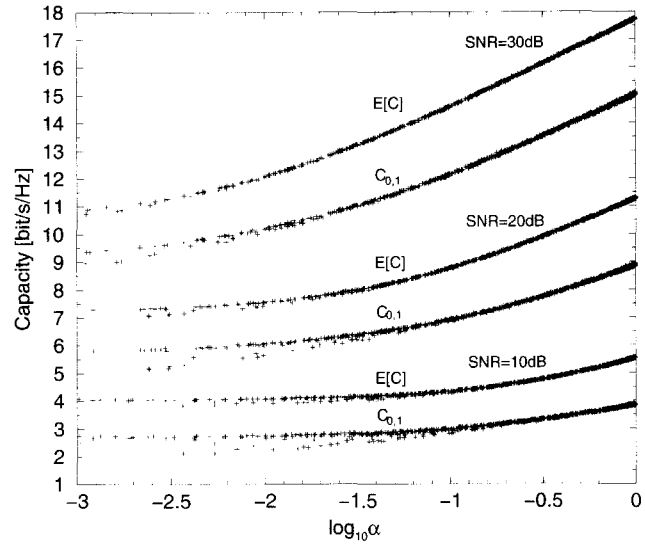

Fig. 14. $\mathbb{E}[C]$ and $C_{0.1}$ vs. α for a (2,2) MIMO system at different SNRs.

we can see an increase in the uncertainty of prediction except, for example, for $\log_{10}(\alpha)$ between -3 and 0 for $P = 30$dB.

Finally, in all these figures, the minimum value of the mean capacity can be predicted by (30). As an example, for a (4,4) system at $P = 30$dB we have $\mathbb{E}[C] = 11.13$ bit/s/Hz. Overall, the α parameter appears slightly better and we recommend this correlation measure as a means of ordering the "overall" correlation in spatially correlated channels.

VI. CONCLUSIONS

In this paper, we have studied the time-variations of the channel in MIMO systems. The analysis has been carried out in terms of LCR's and AFD's of the (instantaneous) capacity, considering both spatially uncorrelated and spatially correlated environments, where the role of correlation at the TX is kept distinct from that at the RX. First, it has been shown that a Gaussian

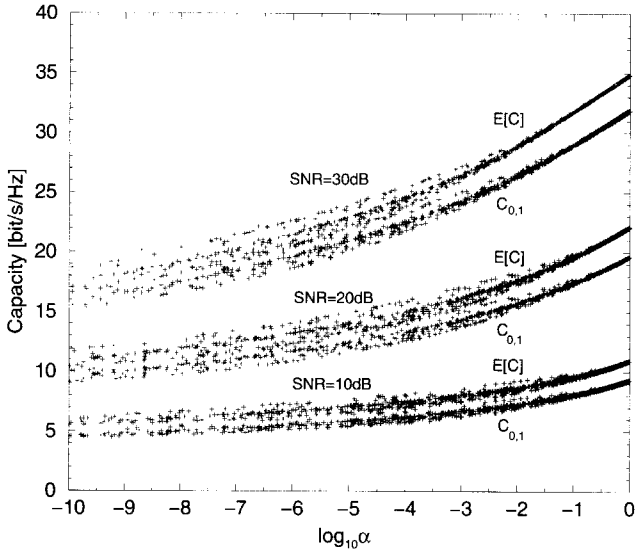

Fig. 15. $\mathbb{E}[C]$ and $C_{0.1}$ vs. α_3 for a (4,4) MIMO system at different SNRs.

first-order approximation is valid even for spatially correlated channels. Then, a Gaussian approximation for the process describing the capacity vs. time has been presented and validated (for moderate numbers of antennas) by means of simulations. It has been shown that LCR's and AFD's are well approximated by that of a Gaussian process. From a numerical point of view, it has been shown that increasing the number of receiving antenna decreases the level crossing rate, and at the same time increases the average duration of capacity fades, for a fixed outage probability. In addition, we have shown that spatial and temporal correlations are separable and that the shape of the capacity ACF is dominated by the shape of the channel ACF. Further, the capacity ACF is relatively insensitive to antenna numbers. The temporal behaviour of the capacity has been modeled by a Gaussian ARIMA process and good agreement observed in the model ACF and PACF compared to the data. The major contribution in the area of spatial correlation is an investigation of the use of a single correlation parameter to predict mean capacity and outage capacity over a wide range of physical scenarios. We suggest two such correlation measures and show their utility in predicting capacity.

APPENDIX A

Defining the standardized capacity values as $\tilde{C} = (C - \mu)/\sigma$ in a discrete time sequence of capacity values we can relate $\tilde{C}(i)$ to $\tilde{C}(i-1)$ as below.

$$\tilde{C}(i) = \rho_c \tilde{C}(i-1) + \sqrt{1-\rho_c^2}\, U(i), \tag{31}$$

where $U(i)$ is an independent normal variable such that $U(i) \sim \mathcal{N}(0,1)$. Note that although (31) has the form of an AR(1) model for the capacity sequence, this analysis does not assume this structure for the entire process. Equation (31) is simply a representation of the bivariate Gaussian relationship which any two successive terms in a Gaussian process satisfy. Hence, the analysis is valid for any Gaussian process. Now, an upcrossing across a level defined by $C = C_T$ is defined by the pair of events: $C(i-1) < C_T$ and $C(i) > C_T$. In terms of standardized values, an upcrossing is also equivalent to the pair of events: $\tilde{C}(i-1) < \tilde{C}_T$ and $\tilde{C}(i) > \tilde{C}_T$ where $\tilde{C}_T = (C_T - \mu)/\sigma$. Hence we have

$$\begin{aligned} LCR(\tilde{C}_T) &= \mathbb{P}\{\tilde{C}(i-1) < \tilde{C}_T, \tilde{C}(i) > \tilde{C}_T\} \\ &= \mathbb{P}\left\{\tilde{C}(i-1) < \tilde{C}_T, U(i) > \frac{\tilde{C}_T - \rho_c \tilde{C}(i-1)}{\sqrt{1-\rho_c^2}}\right\} \\ &= \int_{-\infty}^{\tilde{C}_T} f(x)\left(1 - F\left(\frac{\tilde{C}_T - \rho_c x}{\sqrt{1-\rho_c^2}}\right)\right)dx \\ &= F(\tilde{C}_T) - \int_{-\infty}^{\tilde{C}_T} f(x) F\left(\frac{\tilde{C}_T - \rho_c x}{\sqrt{1-\rho_c^2}}\right)dx, \end{aligned} \tag{32}$$

where $f(x)$ and $F(x)$ are the density and distribution function respectively of the standard Gaussian distribution. This is the desired result.

APPENDIX B

Another approach to the level crossing problem is to use Rice's Formula for the continuous time case. By using standard results from stochastic process theory, it can be shown that, if $\tilde{C}(t)$ is a (standardized) continuous time Gaussian process with ACF $\rho_c(\tau)$, then the upcrossing rate across the level $\tilde{C}_T$ is given by [18], [30]

$$\frac{(-\ddot{\rho}_c(0))^{1/2}}{2\pi} \exp\left(-\frac{\tilde{C}_T{}^2}{2}\right). \tag{33}$$

Some further calculations show that $-\ddot{\rho}_c(0) = Var(d\tilde{C}(t)/dt)$, hence relating the constants to variances of the process rather than the ACF. For the general case, we do not have any analytic results for $\rho_c(\tau)$ or $Var(d\tilde{C}(t)/dt)$ but the form of this result can be easily checked by evaluating $\ddot{\rho}_c(0)$ from the data, or by a simple scaling of the $\exp(-\tilde{C}_T{}^2/2)$ curve. However, for MISO and SIMO systems and for high SNR, following a similar approach developed in Section III-C, we are able to evaluate $\ddot{\rho}_c(0)$ as

$$\ddot{\rho}_c(0) = \frac{d\rho_{\bar{c}}}{d\rho_h} \cdot \ddot{\rho}_h(0) = \frac{2\,{}_2F_1(1,1;n+1;1)}{n\,\psi'(n)} \cdot \ddot{\rho}_h(0). \tag{34}$$

For example, if $\rho_h(\tau) = J_0(2\pi f_D \tau)$ we obtain $\ddot{\rho}_h(0) = -2\pi^2 f_D^2$ and the LCR becomes:

$$f_D \sqrt{\frac{{}_2F_1(1,1;n+1;1)}{n\,\psi'(n)}} \exp\left(-\frac{\tilde{C}_T{}^2}{2}\right). \tag{35}$$

Note also that as for the discrete-time case (32), in the continuous-time case (33) the ACF of the capacity does not play any role, except for values around zero (the second derivative is related to $Var(d\tilde{C}(t)/dt)$).

APPENDIX C

In order to evaluate the term $\mathbb{E}\left[\log_2 X(i) \log_2 X(i-k)\right]$, we need the joint probability density function (p.d.f.) of the two

correlated chi-square r.v.'s $X(i)$ and $X(i-k)$. In order to derive this joint p.d.f., we note that

$$X(i) = \sum_{l=1}^{n} h_l^I(i)^2 + h_l^Q(i)^2, \tag{36}$$

is a sum of zero mean squared Gaussian r.v.'s each with variance 1/2. Also, the underlying Gaussian channels are temporally correlated with ACF

$$R_h(k) = \mathbb{E}[h_l^I(i)h_l^I(i-k)] = \mathbb{E}[h_l^Q(i)h_l^Q(i-k)], \quad \forall l = 1 \cdots n, \tag{37}$$

and normalized ACF $\rho_h(k)$. Hence, from [31, eq. 3.14], we can write the joint p.d.f. of the two correlated central chi-square r.v.'s $X(i)$ and $X(i-k)$ with $2 \times n$ degrees of freedom as:

$$f_{X(i),X(i-k)}(x,y) = \frac{(xy)^{\frac{n-1}{2}}\, e^{-\frac{x+y}{1-\rho_h(k)^2}}}{(1-\rho_h(k)^2)|\rho_h(k)|^{n-1}\Gamma(n)} \cdot I_{n-1}\left(-\frac{2|\rho_h(k)|\sqrt{xy}}{1-\rho_h(k)^2}\right) \quad x \geq 0,\ y \geq 0, \tag{38}$$

where $\Gamma(\cdot)$ is the *gamma function* and $I_n(\cdot)$ is the *n-th order modified bessel function of the first kind* [28, eq. 8.406]. Now, by means of (38) the ACF $R_{\bar{c}}(k)$ can be expressed as

$$\begin{aligned} &\mathbb{E}\left[\log_2 X(i) \log_2 X(i-k)\right] \\ &= \frac{1}{\ln^2(2)} \int_0^\infty \int_0^\infty \ln(x)\ln(y) f_{X(i),X(i-k)}(x,y)\, dxdy \\ &= \frac{1}{(1-\rho_h(k)^2)|\rho_h(k)|^{n-1}\Gamma(n)} \\ &\quad \cdot \int_0^\infty \ln(y)\, y^{\frac{n-1}{2}}\, e^{-\frac{y}{1-\rho_h(k)^2}}\, G(y, \rho_h(k), n)\, dy, \end{aligned} \tag{39}$$

where

$$\begin{aligned} G(y,r,n) \triangleq\ & n^{-1} e^{\frac{r^2 y}{1-r^2}} |r|^{n-1} y^{\frac{n-1}{2}} \\ & \cdot \left[r^2 y\, {}_2F_2\left(1,1;2,n+1;r^2y/(1-r^2)\right)\right. \\ & \left. +(1-r^2)(\ln(1-r^2)+\psi(n))\right]. \end{aligned} \tag{40}$$

Fortunately, after some calculation, the integral (40) can be evaluated in closed form to give:

$$R_{\bar{c}}(k) = \frac{\rho_h^2(k)}{n}\, {}_3F_2\left(1,1,1;2,n+1;\rho_h^2(k)\right) + \psi^2(n), \tag{41}$$

where ${}_3F_2(\cdot;\cdot;\cdot)$ is the *generalized hypergeometric function* [28, eq. 9.14]. This is the desired result.

REFERENCES

[1] J. H. Winters, "On the capacity of radio communication systems with diversity in a radio fading environment," *IEEE J. Select. Areas Commun.*, vol. 5, no. 5, June 1987.

[2] E. Telatar, "Capacity of multi-antenna Gaussian channels," *European Trans. Telecommun.*, vol. 10, pp. 585–595, Nov.–Dec. 1999.

[3] G. J. Foschini and M. J. Gans, "On limits of wireless communications in a fading environment when using multiple antennas," *Wireless Pers. Commun.*, vol. 6, pp. 311–335, 1998.

[4] *IEEE JSAC*, special issue on MIMO systems- part I to appear March 2003, part II to appear June 2003.

[5] Da-Shan Shiu *et al.*, "Fading correlation and its effect on the capacity of multielement antenna systems," *IEEE Trans. Commun.*, vol. 48, no. 3, pp 502–512, Mar. 2000.

[6] D. Chizhik *et al.*, "Multiple-input-multiple-output measurements and modeling in manhattan", *IEEE J. Select. Areas Commun.*, vol. 21, no. 3, pp. 321–331, Apr. 2003.

[7] M. A. Khalighi, K. Raof, and G. Jourdain, "Capacity of wireless communication systems employing antenna arrays, a tutorial study," *Wireless Pers. Commun.*, vol. 23, no. 3, pp. 321–352, Dec. 2002.

[8] A. Abdi and M. Kaveh, "A space-time correlation model for multielement antenna systems in mobile fading channels," *IEEE J. Select. Areas Commun.*, vol. 20, no. 3, pp. 550–560, Apr. 2002.

[9] 3GPP, A standardised set of MIMO radio propagation channels, TSGR#23 R1-01-1179, Jeju, Korea, Nov. 19–23, 2001.

[10] K. Yu, *et al.*, "Second order statistics of NLOS indoor MIMO channels based on 5.2 GHz measurements," in *Proc. IEEE Global Telecommun. Conf., GLOBECOM 2001*, vol. 1, pp. 156–160.

[11] S. Loyka and G. Tsoulos, "Estimating MIMO system performance using the correlation matrix approach," *IEEE Commun. Lett.*, vol. 6, no. 1, pp. 19–21, Jan. 2002.

[12] X. Mestre, J. R. Fonollosa, and A. Pages, IEEE JSAC, special issue on MIMO systems-part I to appear March 2003, part II to appear June 2003.

[13] C. Chuah *et al.*, "Capacity scaling in dual-antenna-array wireless systems," *IEEE Trans. Inform. Theory*, vol. 48, no. 3, pp. 637–650, Mar. 2002.

[14] A. L. Moustakas, S. H. Simon, and A. M. Sengupta, "MIMO capacity through correlated channels in the presence of correlated interferers and noise," *Bell Laboratories Technical Memorandum*, 2001.

[15] C. Martin and B. Ottersten, "Asymptotic eigenvalue and capacity distributions for MIMO channels under correlated fading," in *Proc. ICASSP 2002*, IEEE, 2002.

[16] A. Giorgetti *et al.*, "Level crossing rates and MIMO capacity fades: Impacts of spatial/temporal channel correlation," in *Proc. IEEE International Conf. Commun., ICC 2003*, Anchorage, Alaska, May 11–15, 2003.

[17] A. Giorgetti *et al.*, "Characterizing MIMO capacity under the influence of spatial/temporal correlation," in *Proc. Australian Commun. Theory Workshop, AusCTW 2003*, Melbourne, Australia, Feb. 5–7, 2003.

[18] W. C. Jakes, *Microwave Mobile Communications*, Piscataway, New Jersey, 08855-1331: IEEE Press, IEEE press classic reissue ed., 1995.

[19] Y. Li and X. Huang, "The simulation of independent Rayleigh faders," *IEEE Trans. Commun.*, vol. 50, no. 9, Sept. 2002.

[20] S. H. Simon and A. L. Moustakas, "Optimizing MIMO antenna systems with channel covariance feedback," *IEEE J. Select. Areas Commun.*, vol. 21, no. 3, pp. 406–417, Apr. 2003.

[21] S. A. Jafar, S. Vishwanath, and A. Goldsmith, "Channel capacity and beamforming for multiple transmit and receive antennas with covariance feedback ," in *Proc. Int. Conf. Commun., ICC 2001*, 2001, pp. 2266–2270.

[22] B. M. Hochwald, T. L. Marzetta, and V. Tarokh, "Multi-antenna channel hardening and its implications for rate feedback and scheduling," submitted to *IEEE Trans. Inform. Theory*, 2002.

[23] P. J. Smith and M. Shafi, "On a Gaussian approximation to the capacity of wireless MIMO systems," in *Proc. Int. Conf. Commun., ICC 2002*, 2002, pp. 331–339.

[24] Z. Wang and G. Giannakis, "Outage and mutual information of space-time MIMO channels," in *Proc. 40th Allerton Conf. Commun., Control, and Computing*, Monticello, Illinois, USA, 2002.

[25] M. Chiani, "Evaluating the capacity distribution of MIMO Rayleigh fading channels," in *Proc. IEEE Int. Symp. Advances Wireless Commun.*, Vancouver, 2002.

[26] H. Ge *et al.*, "Statistical characterization of multiple-input multiple-output (MIMO) channel capacity," in *Proc. Wireless Commun. Networking Conf., WCNC 2002*, 2002.

[27] A. Grant, "Rayleigh fading multiple-antenna channels," EURASIP J. Applied Sig. Processing, Special Issue on Space-Time Coding (Part I), vol. 2002, no. 3, pp. 316–329, Mar. 2002.

[28] I. S. Gradshtein and I. M. Ryzhik, *Table of Integrals, Series, and Products*, New York: Academic, 1980.

[29] G. P. Box and G. M. Jenkins, *Time Series Analysis Forecasting and Control*, San Francisco, Holden-Day, 1970.

[30] G. L. M. R. Leadbetter and H. Rootzen, *Extremes and Related Properties of Random Sequences and Processes*, Springer-Verlag, New York, 1983.

[31] M. K. Simon, *Probability distributions involving Gaussian random variables: A handbook for engineers and scientists*, Kluwer Academic Publishers, 2002.

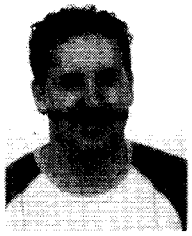

Andrea Giorgetti was born in Cesena, Italy, in 1974. He received the Laurea degree in electronic engineering (with honors) from the University of Bologna, Italy, in July 1999. In 2000, he joined the Department of Electronics, Computer Science and Systems of the University of Bologna, and he is currently working toward his Ph.D. His research interests are concerned with wireless networks, traffic modeling, and performance evaluation of digital communication systems. He is a member of IEEE.

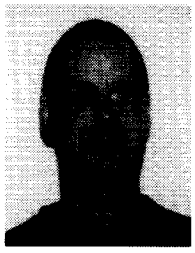

Peter J. Smith received the B.Sc degree in Mathematics and the Ph.D degree in Statistics from the University of London, London, U.K., in 1983 and 1988, respectively. From 1983 to 1986 he was with the Telecommunications Laboratories at GEC Hirst Research Centre. From 1988 to 2001, he was a lecturer in statistics and consulting statistician at Victoria University of Wellington, Wellington, New Zealand. He is currently a senior lecturer in the Department of Electrical and Computer Engineering at the University of Canterbury, Christchurch, New Zealand. His research interests include the statistical aspects of design and analysis for communication systems, especially antenna arrays, mobile radio and MIMO systems.

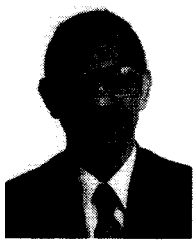

Mansoor Shafi received the B Sc degree in electrical engineering from Engineering University, Lahore, Pakistan and the PhD degree from the University of Auckland, New Zealand in 1970 and 1979 respectively. From 1975 to 1979 he was a Junior Lecturer at the University of Auckland. Since 1979, he has been with Telecom New Zealand where he holds the position of Principal Advisor Wireles Systems. In 1980, he held a Postdoctoral Fellowship at McMaster University, Hamilton ON, Canada. His research interests are in wireless communications. He has published widely in many aspects of wireless communication - mainly in the physical layer. Recently he co-edited the JSAC special issue on MIMO systems. He serves as a NZ delegate to the meetings of ITU-R that are concerned with standardisation of IMT-2000 systems and beyond. He has also been a NZ delegate to WRC 2000 and WRC 2003. Mansoor is an editor for IEEE Transaction Wireless and Kluwer Journal of Wireless Personal Communications.

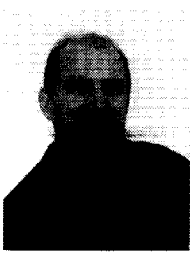

Marco Chiani received the Dr.Ing. degree (summa cum laude) in Electronic Engineering and the Ph.D. degree in Electronic Engineering and Computer Science from the University of Bologna in 1989 and 1993, respectively. Currently he is a Full Professor in the Department of Electronics, Computer Science and Systems (DEIS) at the University of Bologna, where he is also Chair for Telecommunications for the II Faculty of Engineering. His research interests are in the area of communication theory, including interference reduction techniques, channel coding, multiple antenna systems, wireless indoor and mobile radio networks.

In the framework of the European research program Prometheus he worked on short-range millimeter wave communication systems for Advanced Road Transport Telematics. He was involved, for the European Space Agency (ESA-ESOC), in the design and evaluation of channel coding schemes based on Low Density Parity Check Codes for satellite application. He also leads a research group on joint source and channel coding for wireless video systems.

Prof. Chiani chaired and organized several technical sessions at IEEE International Conferences: he was in the Technical Program Committees for the international conferences "IEEE-GLOBECOM97 (Phoenix, USA)," "IEEE-ICC99 (Vancouver, Canada)," "IEEE ICC 2001, Helsinky, Finland," "IEEE ICC 2002, New York". He currently serves as Technical Program Co-Chair for the IEEE Wireless Communications Symposium of ICC 2004.

He is the Editor for "Wireless Communication" for the IEEE Transactions on Communications, and the Chair of the Radio Communications Committee, the IEEE Communication Society.